Articles

Probing the Dynamics of the Silica Nanostructure Formation and Growth by SAXS

Hacène Boukari,[†] J. S. Lin,[‡] and M. T. Harris*,[†]

Chemical Engineering Department and Institute for Physical Science and Technology, University of Maryland, College Park, Maryland 20742, and Solid State Division, Oak Ridge National Laboratory, Oak Ridge, Tennessee 37831

Received May 4, 1997. Revised Manuscript Received October 9, 1997[⊗]

The formation of colloidal silica particles from tetraethyl orthosilicate in several low molecular weight alcohols under base-catalyzed conditions is investigated by small-angle X-ray scattering technique. We measured the changes of the radius of gyration and the fractal dimension as a function of time during growth. We find that, after an induction period, the first particles to form in the solution are mass fractals characterized by their polymeric, open structure. Interestingly, these mass fractals are sizable and could be considered the primary particles. Indeed by undergoing continuous intraparticle densification and further smoothing of the interface, they turn later into the usual compact, nonfractal, stable structures. The stages of growth and transformation, though continuous, cannot be accounted for by the growth models proposed so far.

Introduction

The formation of silica particles has been the subject of extensive investigations for decades because of their wide commercial applications and interesting structural properties. Several methods of synthesis were devised and various techniques were applied to characterize the silica byproducts.[1,2] A well-known route to synthesize silica particles is the Stöber method.[3] In this method highly monodisperse, spherical, compact particles are obtained by hydrolysis and condensation of a tetraalkoxysilane in an alcoholic solution under base conditions. The reaction is described with the following simplified equations:

$$\equiv\mathrm{SiOR} + \mathrm{H_2O} \xrightarrow{\mathrm{OH^-}} \equiv\mathrm{SiOH} + \mathrm{ROH} \qquad (1)$$

$$2\equiv\mathrm{SiOH} \xrightarrow{\mathrm{OH^-}} \equiv\mathrm{SiOSi}\equiv + \mathrm{H_2O} \qquad (2)$$

$$\equiv\mathrm{SiOH} + \mathrm{ROSi}\equiv \xrightarrow{\mathrm{OH^-}} \equiv\mathrm{SiOSi}\equiv + \mathrm{ROH} \qquad (3)$$

where R represents an alkoxy group. Equations 1−3 describe hydrolysis and condensation, respectively.

The Stöber method has been investigated extensively by varying parameters of the reaction (eqs 1 and 2) such as water and base concentrations. These early studies focused on the synthesis and characterization aspects of the silica byproducts. Recently, several investigators have shifted their attention to the study of the mechanisms of formation and growth of these systems as the demand to control and improve the quality of the products and to engineer novel ceramic-based systems increased. For the case of stable colloidal suspensions, it became important that a fundamental understanding of the mechanisms of growth of the particles is essential and crucial to respond to this need. For this purpose numerous studies[4−16] were done and various techniques were applied to investigate both the chemistry and the physical properties of the particles, but more noticeably the dynamics of growth: nuclear magnetic resonance (NMR),[11,13,14] conductivity technique,[9] Raman scattering,[4] dynamic light scattering (DLS),[4,5] transmission electron microscopy (TEM),[13] and small-angle X-ray scattering (SAXS).[15,16]

Despite these extensive investigations, a clear and complete picture for the formation of the particles that

[†] University of Maryland.
[‡] Oak Ridge National Laboratory.
[⊗] Abstract published in *Advance ACS Abstracts,* November 15, 1997.

(1) Iler, R. K. *The Chemistry of Silica*; Wiley: New York, 1979.
(2) Bergna, H. E. *The Colloid Chemistry of Silica*; Bergna, H. E., Ed.; American Chemical Society: Washington, DC, 1990 (and various contributions therein).
(3) Stöber, W.; Fink, A.; Bohn, E. *J. Colloid Interface Sci.* **1968**, *26*, 62.
(4) Matsoukas, T.; Gulari, E. *J. Colloid Interface Sci.* **1988**, *124*, 252.
(5) Matsoukas, T.; Gulari, E. *J. Colloid Interface Sci.* **1989**, *132*, 13.
(6) Harris, M. T.; Brunson, R. R.; Byers, C. H. *J. Non-Cryst. Solids* **1990**, *119*, 397.
(7) Harris, M. T.; Basaran, O. A.; Byers, C. H. *Ceramics Powder Sci. III* **1990**, *12*, 119.
(8) Bogush, G. H.; Zukoski IV, C. F. *J. Colloid Interface Sci.* **1991**, *142*, 19.
(9) Bogush, G. H.; Zukoski, C. F. *J. Colloid Interface Sci.* **1991**, *142*, 1.
(10) Harris, M. T. Ph.D Dissertation, University of Tennessee, 1992, unpublished.
(11) van Blaaderen, A.; van Geest, J.; Vrij, A. *J. Colloid Interface Sci.* **1992**, *154*, 481.
(12) van Blaaderen, A.; Kentgens, A. P. M. *J. Non-Cryst. Solids* **1992**, *149*, 161.
(13) Bailey, J. K.; Mecartney, M. L. *Colloids Surf.* **1992** *63*, 151.
(14) Lee, K. T.; Look, J. L.; Harris, M. T.; McCormick, A. V. *J. Colloid Interface Sci.*, in press.
(15) Brinker, C. J.; Keefer, K. D.; Schaefer, D. W.; Assinik, R. A.; Kay, B. D.; Ashley, C. S. *J. Non-Cryst. Solids* **1984**, *63*, 45.
(16) Keefer, K. D.; Schaefer, D. W. *Phys. Rev. Lett.* **1986**, *56*, 2376.

S0897-4756(97)00287-1 CCC: $14.00

spans the full time range, from initiation of synthesis to the final stage of stable particles, has not yet emerged. There are still open questions regarding the mechanisms of growth. A good illustration of this point is the contrasting and different growth models that have been proposed so far, in particular, the monomer addition[5] based on LaMer model and controlled aggregation.[8,9] In these models as well as other variations[6,7,11,13] an ever elusive "primary" particle is always mentioned. However, besides the excellent suggestive cryo-TEM work of Bailey et al.,[13] the primary particle has not been observed. Thus, elucidating the earliest stages of the formation of nanostructures is the key to unraveling the mechanisms that govern the formation of silica particles. SAXS technique is an excellent tool for probing the formation of such nanostructures and offers several advantages over the cryo-TEM technique. Mainly, SAXS measurements are nonintrusive and are easy to perform.[17,18] More appealing is the ability to elucidate the nanostructure as well as measure the size and size distribution of the scattering particles.

In this paper we report in situ, time-dependent SAXS measurements obtained from the scattering of particles that are formed during the base-catalyzed hydrolysis and condensation of tetraethyl orthosilicate (TEOS) in an alcoholic solvent (Stöber method[3]). Under the right reactant ([TEOS] and [H_2O]) and catalyst ([NH_3]) concentrations, SAXS can be used to study the continuous formation of the nanostructures from the monomer to the final compact particles as TEOS undergoes base-catalyzed hydrolysis and condensation reactions in low molecular weight alcohols. Such were the conditions that were explored in our investigations.

We analyzed both the Guinier and power-law regimes of the time-dependent data and determined the changes of the radius of gyration and the fractal dimension of the particles during growth. The measurements show, first, that the mechanism of the formation of the silica particles is nucleation-and-growth. Second, the first structures observed initially are of polymeric, fractal nature. Third, these low-density structures densify continuously until becoming compact with smooth interfaces as commonly observed.

The chemistry of the base (NH_3)-catalyzed hydrolysis and condensation of TEOS in ethanol has been studied.[1−3] Recently, more extensive studies have been done by Lee et al.[14] Remarkably, these investigations show that, preceding condensation, only unhydrolyzed monomers ($Si(OC_2H_5)_4$) are present in the solution and the first hydrolysis product is $Si(OH)(OC_2H_5)_3$. Condensation proceeds then either by oxolation, the release of water during the reaction of two silanol groups, or by alkoxolation, which is the release of alcohol by the reaction of a silanol group with a silicon−alkoxyl ligand. It is during these condensation reactions that oligomeric and polymeric moieties are formed.

Small-Angle X-ray Scattering of Particles

In scattering experiments, one measures the scattered-intensity profile of the scattering sample as a function of the scattering angle, θ. The measured profile is then compared with the calculated static structure factor, $S(q)$, which is the Fourier transform of the two-point density−density correlation function of the scattering system.[17−22] Here the amplitude of the wavevector is given by $q = 4\pi \sin(\theta/2)/\lambda$ with $\lambda = 1.54$ Å being the wavelength of the X-ray beam. Expressions for $S(q)$ were derived for several simple systems such as spherical particles, disks, and rods.[17] For complex and random systems, the concept of fractal geometry has been applied to interpret some of the measured scattering profiles.[19−22] In the fractal description the important parameter is the fractal dimension, D, that quantifies the way in which a property of the fractal object such as the mass, M, in mass fractals or the surface area, A, in surface fractals increases with length or radius, r.

For mass fractals, which can be pictured as open, polymeric, low-density structures, the mass M is scaled as[20−22]

$$M \sim r^{D_m} \tag{4}$$

where D_m is in general a noninteger number ranging $1 < D_m < 3$. If $D_m = 3$, we recover the Euclidean (nonfractal) description of the mass (in three dimensions the mass of a sphere scales as the radius cubed). In contrast surface fractals have uniform cores but open surface structures with an area, A, described by[20−22]

$$A \sim r^{D_s} \tag{5}$$

Here D_s is defined as the corresponding fractal dimension of the surface and, similarly to D_m, D_s is in general a noninteger number in the range $2 < D_s < 3$. If $D_s = 2$, we obtain the classical function relating surface and length (the area of the surface of a sphere scales as the radius squared).

The fractal dimension of a particle can be determined from its scattering profile, $S(q)$, by analyzing the power-law regime covering the range $R_g^{-1} \ll q \ll a^{-1}$. Here R_g is the radius of gyration of the particle and a is the size of the smallest units building the fractal structure. In this regime it has been shown that $S(q)$ is of a power-law form:[19−22]

$$S(q) \sim q^{-\alpha} \tag{6}$$

where the exponent α is related to the fractal dimension of the scattering structures. For mass fractals, one can show that $\alpha = D_m$ and $1 < \alpha < 3$ in a 3-dimensional space. In contrast, we have $\alpha = 6 - D_s$ for surface fractals. If $D_s = 2$, we obtain the well-known Porod's law ($S(q) \sim q^{-4}$) for nonfractal structures with smooth interfaces. More remarkable is the result that for surface fractals we have $3 < \alpha < 4$, larger than the values of mass fractals.

Thus, by measuring the exponent α of the power-law regime, one can determine the nature of the structure of scattering particles. Depending on the value of the

(17) Guinier, A.; Fournet, G. *Small Angle Scattering of X-rays*; Wiley: New York, 1955.
(18) Glatter, O., Kratky, O, Eds. *Small-Angle X-ray Scattering*; Academic Press: London, England, 1982.
(19) Schaefer, D. W.; Keefer, K. D. *Phys. Rev. Lett.* **1984**, *53*, 1383.
(20) Schmidt, P. W. In *The Fractal Approach to Heterogeneous Chemistry: Surface, Colloids, Polymers*; Avnir, D., Ed.; John Wiley & Sons: Chichester, England, 1989.
(21) Schmidt, P. W. *J. Appl. Crystallogr.* **1991**, *24*, 414.
(22) Schmidt, P. W. In *Modern Aspects of Small-Angle Scattering*; Brumberger, H., Ed.; Kluwer Academic Publishers: The Netherlands, 1995.

Table 1. Sample Compositions and SAXS Configuration Used To Measure the Scattering Profile

sample	[H_2O] (mol/L)	[TEOS] (mol/L)	[NH_3] (mol/L)	solvent	SAXS configuration
E1	2.2	0.5	0.1	EtOH	2-m
E2	1.1	0.5	0.1	EtOH	2-m
E3	2.2	0.5	0.04	EtOH	5-m
M1	1.1	0.5	0.1	MeOH	2-m
M2	1.1	0.5	0.05	MeOH	2-m
P1	1.1	0.5	0.05	PrOH	5-m

exponent α, it is possible to distinguish whether we have mass or surface fractals or just nonfractals.

In addition to the fractal dimension, one can also measure R_g from the Guinier regime ($qR_g \ll 1$) of the scattering profile. In the limit of low-q $S(q)$ is approximated by a Gaussian function:[17]

$$S(q) = I_0 e^{-q^2 R_g^2/3} \tag{7}$$

The changes of R_g provides information about the size of the scattering fractals and the degree of overlap and interaction between the scattering structures.

Sample Preparation and Experimental Setup

The silica particles were prepared by hydrolysis and condensation of TEOS in an alcoholic solution with NH_3 as a base-catalyst. Several alcohols were used: 200-proof ethanol (EtOH) from Pharmaco Products, Fisher-grade 2-propanol (PrOH) from Fisher Scientific, and methanol (MeOH) from J. T. Baker. Both concentrated ammonium hydroxide (30% NH_3) and TEOS (99% purity) were purchased from Aldrich Chemical Co. The 18.2 MΩ water was produced by a Millipore filtering system. We used the following densities (ρ) and molecular weights (m) to calculate the molar concentrations of the various chemicals: $\rho_{TEOS} = 0.93$ kg/L, $m_{TEOS} = 208.3$ g/mol, $\rho_{EtOH} = 0.78$ kg/L, $m_{EtOH} = 46.07$ g/mol, $\rho_{MeOH} = 0.79$ kg/L, $m_{MeOH} = 32.04$ g/mol, $\rho_{PrOH} = 0.80$ kg/L, $m_{PrOH} = 60.11$ g/mol, $\rho_{H_2O} = 1$ kg/L, $m_{H_2O} = 18$ g/mol, $\rho_{NH_3} = 0.89$ kg/L (30% aqueous solution), and $m_{NH_3} = 14.7$ g mol/L (per liter of solution).

The reaction was initiated by mixing vigorously TEOS−alcohol solution and water−ammonia−alcohol solution in a cleaned and well-rinsed bottle. The SAXS cell was immediately filled with the mixture and placed in the X-ray setup (usually within 15−20 min). Transmission measurements of the different samples indicate variations in the spacing between the Kapton windows from one sample to another. In all our samples the molar concentration of TEOS was fixed to [TEOS] = 0.5 M, whereas the molar concentrations of water and ammonia were varied to slow the growth rate of the particles. We list in Table 1 details of the various samples discussed here.

The SAXS measurements were obtained at the SAXS Facilities at Oak Ridge National Laboratory. The SAXS setup is of the pinhole geometry type, and no desmearing of the data was therefore needed.[23] The measurements were taken at room temperature using a 4 kW power incident beam of wavelength of 1.54 Å (Cu Kα), under low vacuum (<50 mTorr). The 2-dimensional (20 × 20 cm^2 area) position-sensitive proportional detector was placed at two different distances away from the sample, giving two different q ranges. The 5.119-m distance was used mostly to probe the Guinier regime and sometimes a part of the power-law regime of the particles. In this configuration the wavevector range is $0.043 < q < 1.05$ nm^{-1}. Then, we moved the detector within 2.119 m from the sample, focusing specifically on the power-law regime. In this configuration the q range is $0.10 < q < 2.50$ nm^{-1}.

Experimental Results

We monitored the formation and growth of the silica particles by measuring the scattered intensity profiles at small angles with respect to normal incidence at various times following the mixing of the chemical components. The collection time of the scattered intensities was varied depending on the average count rate. Here the average count rate is estimated from the total count measured over a time period (∼9000 s) by the 4000 detection elements distributed over the 2-dimensional detector. For all samples the average count rate started at about 32−37 counts/s (dark count ∼13 counts/s), and the collection time was set to 1800 s. When the scattering signal became stronger, we reduced the collection time to 1200 s. All the data were corrected for the background distribution by using the intensity profile measured for pure alcohols. If there is no difference between the intensity profile of the pure alcohol and the first measured intensity profile of the reacting sample (EtOH solvent in particular), we preferred to use the first intensity profile as a background.

We start by showing in Figure 1 some of the SAXS intensity profiles measured at various times following the initiation of hydrolysis and condensation in samples prepared in ethanol (E1, E2, and E3 in Table 1). The transmitted intensity for these samples was: $T \simeq 0.37$. For comparison we show in Figure 2 similar SAXS measurements obtained from samples prepared in methanol (M1 and M2 in Table 1). The transmission in these samples is 0.20 (M1) and 0.23 (M2). We also obtained similar SAXS measurements with propanol as solvent (P1 in Table 1 with transmission close to 0.31). To reduce the number of figures, we just discuss the results determined from the propanol measurements.

From Figures 1 and 2 two interesting features can be immediately noticed: the increase of the scattering intensity and the change of the slope in the high q regime of the scattering profile as a function of time. One can first relate the increase of intensity to changes in the size of the particles as well as an increase of the total number of particles. The change in the slope of the intensity in the log−log plot at high q indicates changes in the structure of the particles.

We fit the low-q data with the Gaussian function of eq 7 and determined R_g. We note that because of the relatively large size of the structures prepared in ethanol (even in the initial stage) R_g is determined from measurements obtained with the long configuration (sample E1). In Figure 3 we show the changes of R_g as a function of time for the samples E1, M1, M2, and P1. (E2 and E3 are not analyzed as the q range covers partially the Guinier regime.) Here t denotes the time distance from the initiation of the reaction ($t = 0$ is the mixing time of the chemical components). As expected, R_g increases as a function of time, indicating the growth of the particles. Remarkably, one can notice that while the size of the particles prepared in ethanol and propanol have almost the same size, the particles prepared in methanol tend to be small, a factor of 2 difference in size.

It is difficult, however, to determine the exact shape and the nature of the structure of these particles; R_g yields information only about the presence of "structures". The power-law regime provides more information about the structure of the scattering particles. We least-squares fit the data with the power law of eq 6 in the appropriate q range with α being a fitting parameter. In Figure 4, we plot the changes of the exponent

(23) Wignall, G. D.; Lin, J. S.; Spooner, S. *J. Appl. Crystallogr.* **1990**, *23*, 241.

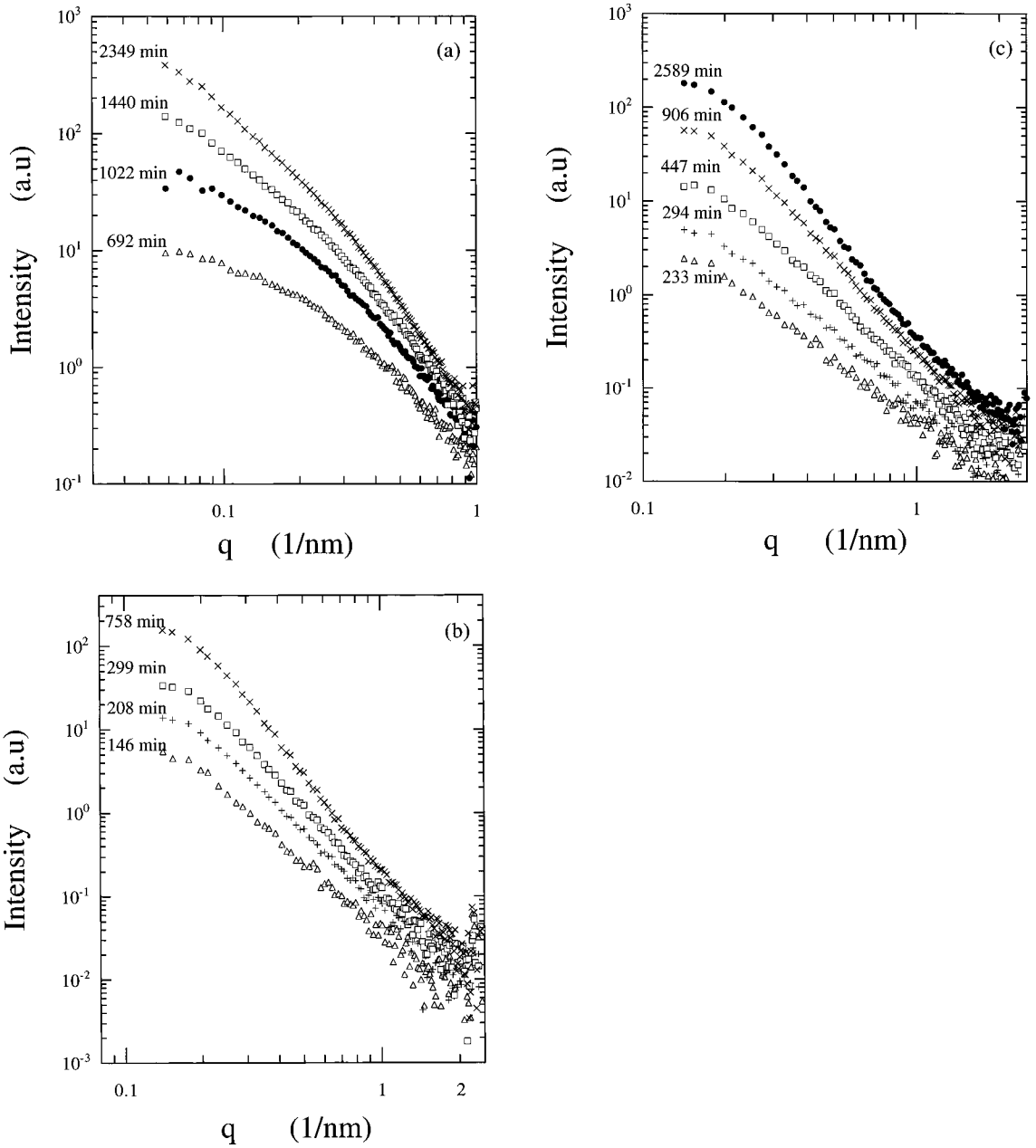

Figure 1. Measured scattered intensities are plotted against wavevector of samples: (a) E1, (b) E2, (c) E3 in Table 1. Each curve is labeled with the time in minutes following the mixing of the chemical components of the respective samples.

α of some of the samples as a function of time. In the same figure, we indicate the corresponding fractal structure as either mass fractal (α < 3) or surface fractal (α > 3). We notice that the rate of changes of α depends again on the chemical composition of the sample; higher concentrations of water induce fast changes in the exponent (contrast α of E2 and M1 with that of E3 and M2, respectively) and low concentrations of [NH_3] slow the kinetics of growth (contrast α changes of E1 with that of E3). Interestingly, one can notice that the shapes of α vs t curves in Figure 4 are identical, and only a shift in time distinguishes the curves. This suggests that the formation and growth processes are the same for all the samples.

Finally, we plot in Figure 5 the changes of the scattering intensity of the samples at a fixed low q_f value as a function of time: $q_f = 0.090$ nm^{-1} for E1, $q_f = 0.084$ nm^{-1} for P1, and $q_f = 0.178$ nm^{-1} for M1 and M2. A similar behavior is obtained if the fitted value I_0 ($I(q\rightarrow 0)$) of eq 7 is plotted; it is more accurate to plot the measured scattered intensities at a known q value than I_0 since the Gaussian function is just an approximation for the behavior of the scattering intensity at low q. In Figure 5 we notice that there is a delay time, Δt, where no significant changes in the scattering intensity is observed. This delay time depends on the solvent and the concentrations of water and catalyst. We have Δt (E1) < 330 min, Δt (M1) < 40 min, Δt (M2) < 40 min, and Δt (P1) < 200 min. This delay time can be related to the induction time observed in turbidity experiments performed with similar growth processes. We note that since our interest is in the early stage of growth, we usually terminate the experiments as soon as the measured exponent α hits the value 4 (Porod's law). Therefore, some of the data (E1, P1, and M2) shown in Figure 5 span only a short period of the time, a part of the early and intermediate regimes (we expect the curves to level off when the equilibrium state is approached). In contrast, the intensity appears to have leveled off for sample M1.

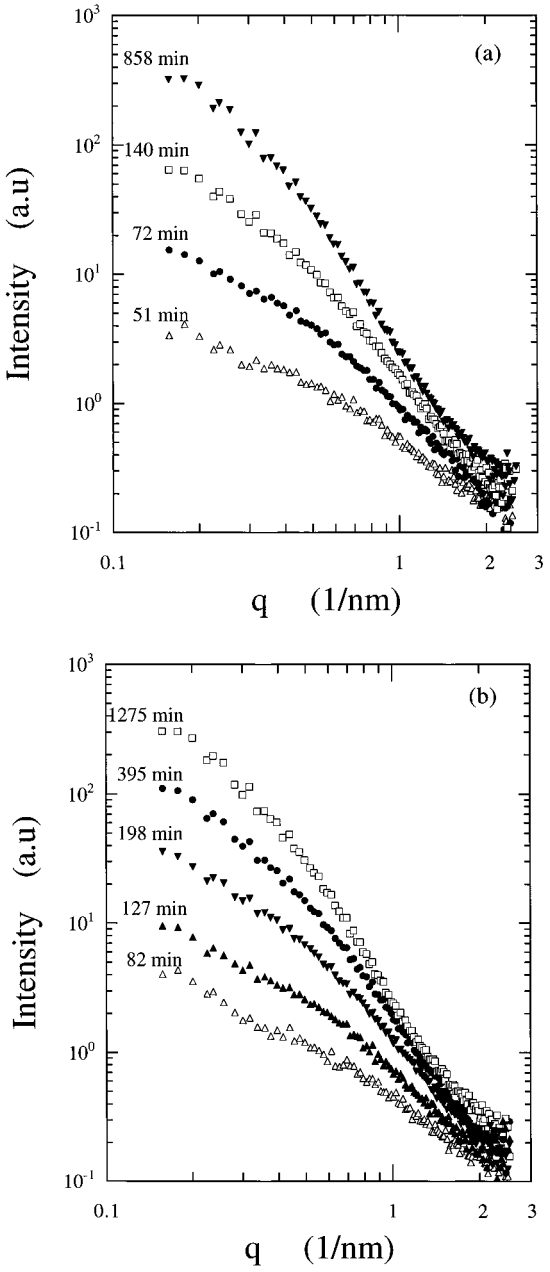

Figure 2. Measured scattered intensities are plotted against wavevector of samples: (a) M1, (b) M2 in Table 1. Each curve is labeled with the time in minutes following the mixing of the chemical components of the respective samples.

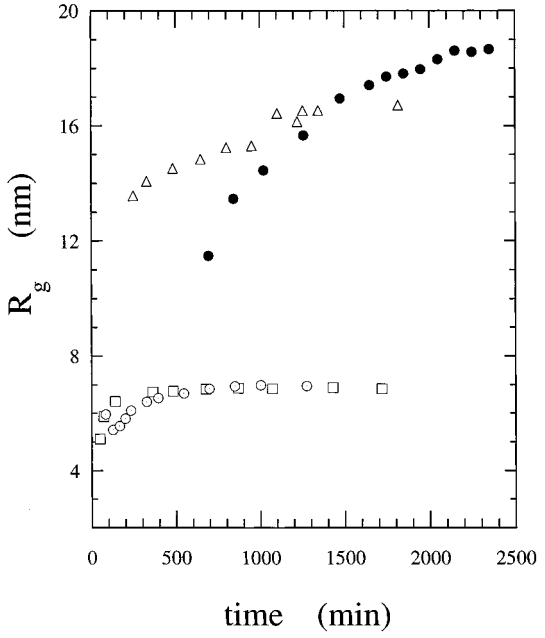

Figure 3. Measured radius of gyration of various samples (Table 1) is plotted as a function of time following the mixing of the chemical components: P1 (△), E1 (●), M1 (□), and M2 (⊙).

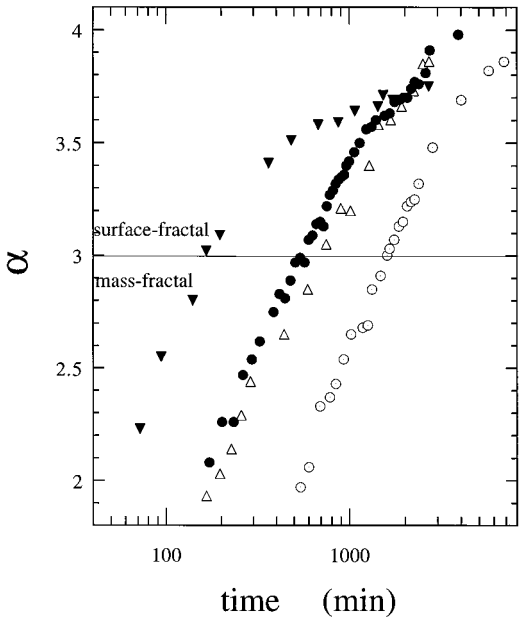

Figure 4. Exponent α determined from eq 6 plotted as a function of time: E1 (⊙), E2 (●), E3 (△), and M1 (▽).

Polydispersity in the Scattering Sample

In our analysis of the data we have made an implicit assumption that the scattering system is monodisperse. Here monodispersity is assumed not only for the size of the particles but also for the fractal structure of the particles. That is, all the particles have the same fractal dimension and the same size. However, our chemically reactive samples, especially with the low concentrations of water and ammonia, may not satisfy this assumption as new particles with different size and fractal dimension are continuously formed during the experiment and those that exist undergo intraparticle structural changes as well as increase in size. It is only when the reactions are completed ($t \rightarrow \infty$, final equilibrium state) that one may test the validity of the monodispersity assumption. For our time-dependent measurements the R_g values and α values determined here (Figures 3 and 4) represent average values at the corresponding time (a full analysis of this question will presented elsewhere[24]).

The monodispersity of the particles at later stages is checked with the TEM technique. Figure 6 is a TEM micrograph of the final silica particles that were produced by the reaction of [TEOS] = 0.5 M, [H_2O] = 2.2 M, and [NH_3] = 0.1 M in ethanol. The silica particles have a diameter of 30−50 nm and are fairly monodisperse. The average radius of gyration of silica particles produced in ethanol was approximately 18 nm (Figure 3). For spherical particles of radius R we have $\sqrt{5/3}R_g$.[17,18] Thus, the average diameter of the spheres should be approximately 46 nm which is in very good

(24) Boukari, H.; Harris, M. T., to be published.

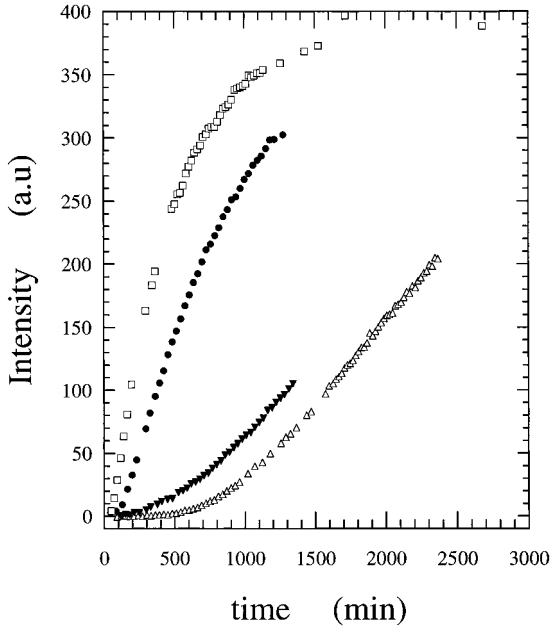

Figure 5. Changes of the scattering intensity at low-q wavevectors shown as a function of time for the samples: E1 (△), P1 (▽), M1 (□), and M2 (●).

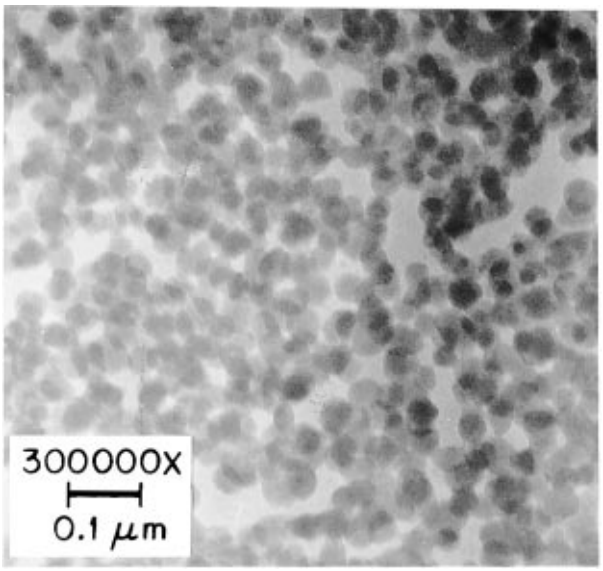

Figure 6. TEM micrograph of sillica particles produced by Stober method.

agreement with the TEM results where the average diameter of 50 particles was 40 nm. It is also observed that the particles agglomerated upon drying since dynamic light-scattering measurements yielded an average hydrodynamic diameter of approximately 40 nm for a suspension of these particles in the reaction solution.[25]

One important question we should address is the effect of a distribution of sizes on the measured exponent α. It has been suggested that polydispersity can yield a lower apparent exponent α even though the particles are nonfractals. This is especially the case for a power-law size distribution of particles, where the possible apparent exponent has been calculated.[21,22] While we are not ruling out the presence of a size distribution of particles (in fact, it is necessary to fully explain the increase in the intensity), we are ruling out the possible presence of a wide distribution of nonfractal particles and in particular compact, spherical particles. First, if we assume that the initial particles are not fractals (especially, mass fractals) but rather smooth compact spherical particles with varying sizes, we find that the initial size distribution shows a single maximum peak around a radius $R \sim 10$ nm with a full width at half-maximum (fwhm) < 10 nm.[25] This fwhm becomes smaller as a function of time, sharpening the distribution. More importantly, this fwhm is too small to account for the measured α values; the variation of sizes should be an order of magnitude to have a significant effect on the exponent α.[26] Second, if a significant concentration of compact, smooth particles are formed from the beginning, one should expect Porod's law ($1/q^4$) in the high-q range ($qR_g \gg 1$),[27] a law characteristic of a smooth interface. We observed this power law only in the later stages of growth. Finally, our observations are further supported by the observations of Bailey et al.[13] In their cryo-TEM micrographs they observed only a narrow size distribution of silica particles in their samples in the early stage of growth.

Discussion

Three points should be emphasized about the measurements described above: (1) the changes of the intensity as a function of time, (2) the change of the exponent α, and (3) the relatively large R_g of the particles that appeared initially in the sample.

Nucleation−Condensation. Figure 5 shows that within the resolution of the instrument the route for the formation of the particles is by nucleation and growth. During the delay time, Δt, or induction period one can think that hydrolysis of TEOS molecules is the dominant reaction. Δt depends on several factors: concentration of water, concentration of catalyst, and solvent. Certainly, one expects that low concentrations of water and catalyst tend to prolong Δt as hydrolysis is slowed. However, for the same concentrations of water and catalyst the delay time (induction time) is strongly dependent on the solvent although the same chemical reactions occur in the system.

If we turn to the recent NMR results to figure out the type of monomers forming during Δt, Lee et al.[14] show, interestingly, that for low concentrations of water, the first hydrolyzed TEOS molecules (the monomers) are partially hydrolyzed. That is, not all four ethoxy groups attached to Si are hydrolyzed at once. So, when a critical concentration of monomeric hydrolyzed TEOS molecules—supersaturation concentration is reached—condensation−nucleation proceeds with these monomers, resulting in the formation of structures that are initially of polymeric nature (several ethoxy groups on Si will still be present and have to be removed for complete hydrolysis). The fractal nature of these first particles is confirmed by the power-law behavior of the scattering data at high-q shown in Figures 1b, 1c, 2a, and 2b and the values of the α exponent determined

(25) Boukari, H. Dolan, J.; Singhal, A.; Long, G. G.; Harris, M. T., to be published.

(26) Beaucage, G. private communication.

(27) Teixeira, J. In *On Growth and Form: Fractal and Non-Fractal Patterns in Physics*; Stanley, H. E., Ostrowsky, N., Eds.; Martinus Nijhoff Publishers: Dordrecht, 1986.

from this regime (Figure 4). Remarkably, the initial α values ($\alpha \simeq 2$) indicates that these particles are mass fractals.

Transition from Mass Fractals to Nonfractals. The change of α shown in Figure 4 indicates that the structure of the particles is continuously changing: from mass fractal ($2 < \alpha < 3$), to surface fractal ($3 < \alpha < 4$), to finally nonfractal particles with smooth interfaces ($\alpha = 4$). The rate of changes depends on the concentration of water [H_2O], the concentration of [NH_3] catalyst ([TEOS] being fixed), and the solvent. The initial structures observed in all samples are mass fractals, which are characterized by their polymeric, noncompact structures.

As hydrolysis continues and the remaining ethoxy groups are removed from the particles by "intraparticle" densification, the polymeric structures undergo densification. This process can be thought of as a filling process of the available bonds (sites) of the polymeric structures. As a result, the fractal dimension $D_m = \alpha$ increases continuously. If most of the inner available bonds are filled, hydrolysis continues on open bonds at the sites available at the outer interface with the solvent. At this stage, the dominant scattering signal comes from the outer still random structures interfacing with the solvent, turning the polymeric, mass fractals into surface fractals and yielding $\alpha > 3$. The surface is then described by the surface fractal with the fractal dimension $D_s = 6 - \alpha > 2$.

The later stage is dominated by a "smoothing" process as hydrolysis continues. This would be characterized by further hydrolysis of partially hydrolyzed TEOS molecules already attached at the surface of the particles and addition of new but noncompletely hydrolyzed TEOS molecules. Because the size of the particles is big ($R_g \sim 7$ nm for MeOH and $R_g \sim 18$ nm for PrOH and EtOH) the surface appears smooth at this length scale ($D_s \simeq 2$ or $\alpha \simeq 4$), giving Porod's law. We note here that the size increases slowly as the particles become stable in the solution and aggregation between particles is not considered.

Initial Size and the Role of the Solvent. It appears that the initial mass fractals are the smallest structures to form in the matrix solution following the mixing of the chemical components. In all our samples, the initial R_g observed depends particularly on the solvent and not on the concentration of water and ammonia. In methanol $R_g \sim 5$ nm, whereas the other solvents (propanol and ethanol) yield a larger size ($R_g \sim 10$ nm). At the length scale probed by our experiment and within the time resolution used, we did not observe either high- or low-density primary particles of smaller sizes that could have aggregated and grown to form the nano, fractal structures. This result corroborates previous observations made by Bailey et al.[13] using the cryo-TEM technique. First, they did observe low-density particles of size >12 nm in their cryo-TEM micrographs in the early stage of growth. Second, they did not observe particles of smaller sizes at any stages during growth.

However, on the basis of further observations, Bailey et al.[13] suggest that the initial mass fractals (polymeric-like) grow until reaching a nonsustainable size. At this point, for entropic energy considerations the ramified or polymeric particle collapses to a more compact and dense state. Then, the particle size increases by addition of small particles at the surface boundaries. If this scenario is correct, one should observe this sudden collapse at the transition from mass fractal to surface fractal ($\alpha < 3$ to $\alpha > 3$) as a compact core forms in the surface fractal. To check this point, we paid particular attention to the SAXS measurements obtained at the transition from mass fractal to surface fractal and analyzed thoroughly the Guinier regime. Within our resolution and noise level we do not find any sudden changes of R_g. Instead, R_g changes smoothly and continuously as Figure 3 shows. This result suggests further that continuous hydrolysis is responsible for the transition from mass fractal to surface fractal.

Possible Mechanisms of Growth. To put the present results in perspective, it is essential to separate the mechanisms of formation of the individual fractal structure from the processes of intraparticle densification, smoothing of the interface, and increase in size of the existing particles. It appears that the time scales for such mechanisms and processes are different. Following the induction period the first sizable mass fractals form in a short period of time (short compared with the collection time of the SAXS measurements). Then, the ensuing slow processes of intraparticle densification, smoothing of the interface, and increase in size take place in hours to weeks depending on the concentrations of water and catalyst and the solvent.

Formation of the Nanostructure. In an earlier work Keefer[28] and Schaefer and Keefer[28,29] focused on the nanostructure of the particles and proposed the poisoned Eden model, a modified version of the traditional Eden model. Their goal is to explain their SAXS measurements which show that, with relatively low concentrations of water, the structure of the particle is fractal (more precisely surface fractal). In the poisoned Eden model, several sites of growth are "killed" to mimic the incomplete hydrolysis assumed in the reaction and during growth. The simulation indeed yields final structures that are not completely compact (to be contrasted with the compact structures obtained with the traditional Eden model).

However, in their analysis of the measurements, Keefer and Schaefer[29] assumed that the measured scattering profiles represented the scattering profiles of a system in its final stage (close to its final structure) as hydrolysis was very slow due to the low concentration of the base catalyst. Thus, they obtained low fractal dimensions for their samples. Using the present results we can argue that their measurements were taken in an intermediate regime, a very slowly evolving state. So, even if the correct initial distribution of monomers with different functionalities is used, the "poisoned" Eden model may be appropriate to describe the dynamics of growth in the early stage (mass fractal) but cannot account for the rest of the growth (intraparticle densification and smoothing) leading to the final compact particles.

To understand the dynamics of growth of the initial fractal structures, one can consider comparing the

(28) Keefer, K. D. In *Better Ceramics through Chemistry*; Mater. Res. Soc. Symp. Proc.; Brinker, C. J., Clark, D. E., Ulrich, D. R., Eds.; 1986, Vol. 73.

(29) Schaefer, D. W.; Keefer, K. D. In *Better Ceramics through Chemistry*; Mater. Res. Soc. Symp. Proc.; Brinker, C. J., Clark, D. E., Ulrich, D. R., Eds.; 1986, Vol. 73.

measured value of the fractal dimension with that calculated from available growth models that yield fractal structures. One can then surmise on the appropriate growth model. Typical models are diffusion-limited aggregation (DLA) and reaction-limited aggregation (RLA) that produce such fractal structures.[30] In our experiments the measurements are taken in a nonequilibrium state, and therefore it is not obvious to make a direct comparison with values calculated from a final equilibrium state ($t \rightarrow \infty$). We should mention, however, that the smallest fractal dimension measured initially is close to 2, and this value is within error comparable with $D \simeq 2.1$ calculated for RLA model in 3-dimensional space. This suggests that the growth of the first mass fractals proceeds by RLA though in a short time as mentioned above. We emphasize that this observation needs further conclusive measurements.

Primary Particles for the Growth Models. Several growth models for the silica particles prepared by the Stöber method have been reported in the literature. The main goal of these models is to identify mechanisms of growth that appropriately favor the production of compact, spherical, monodisperse silica particles in equilibrium at the end ($t \rightarrow \infty$). Noticeably, we mention the monomeric-addition model by Matsoukas et al.[4,5] and controlled aggregation model by Bogush et al.[8,9]

Matsoukas et al.[4,5] suggest that the formation and growth of the particles follow closely though not exactly the LaMer nucleation-growth model.[31,32] In their model particle nucleation is the result of the reaction between two reactive monomers formed by hydrolysis. Subsequently, particles are grown by addition of monomers, and this growth process can be described by the general kinetic equations applied to chemical reactions. Because of the addition mechanism the size distribution of the particles remains very narrow during growth and until the end of process. Further the final particle size is determined by the balance between the monomer addition and nucleation, and as such, the particle growth is rate-limited by hydrolysis.

In contrast Bogush et al.[8,9] proposed a nucleation and controlled-aggregation mechanism in which primary particles (sometimes called subparticles) are formed following the induction period and then aggregate to form larger stable particles. Because of a controlled aggregation mechanism, only a narrow distribution of sizes is favored and ultimately appears at the end of the process. This controlled aggregation is described as follows: once the aggregates or subparticles have reached a certain size and thereby gained colloidal stability, the growth proceeds favorably by aggregation of small particles with these large particles and no aggregation between the large particles is allowed. As such the final equilibrium distribution and the size are determined by parameters such as surface charges.

In addition to these extreme models, other models were also developed to either remedy some of the deficiencies of these two models or explain new experimental observations.[6,7,10,11,13] However, none of these models has specifically addressed the nature of the so-called primary particles that are formed by nucleation and critically investigated this nature experimentally. The present results show that the initial particles have polymeric-structure (mass fractals) and are surprisingly sizable. Furthermore, these mass fractals appear to represent the nucleating backbones or seeds used to build the compact and stable particles observed later in the growth. And no smaller particles (subparticles) are present in the solution. Simply, they are the primary particles.

For comparison with the previously discussed models we first note that we have suggested the aggregation-polymerization mechanism only in the formation of the initial mass fractals and new particles. Here the aggregative monomers are the partially hydrolyzed TEOS molecules. So, contrary to the Bogush et al. model there is no need to assume the existence of subparticles in the solution, and a controlled aggregation mechanism is not necessary to account for the monodispersity of the particles (final equilibrium particles). We should point out that before this equilibrium is reached, there is a distribution of particles of various sizes and fractality. Indeed, careful analysis of the SAXS measurements show deviations from one-single power-law in the scattering data obtained at later times (see intensity profiles at later times in Figures 1 and 2). This behavior can be attributed to the appearance of a distribution of particles of various fractal dimension as a result of continuous nucleation and formation of new particles that have low fractal dimension, likely to be mass fractals with $D_m \sim 2$ as in the initial particles.

The subsequent growth of the particles is controlled by addition of monomers (partially hydrolyzed TEOS molecules), a result consistent with the model proposed by Matsoukas et al. However, it is unclear at this point to perform similar calculations with the general kinetic equation since the changes in the SAXS measurements can be caused by several factors. In contrast to light-scattering measurements, the changes in the scattered intensities during nucleation and growth is related not only to changes in the number and size of the particles but also to changes in the fractal structure. It is only in the case of compact particles that $I(q=0)$ is related to the ratio of the surface to the total volume of the particles. This condition may be applicable with high concentrations of water and/or catalysts in which hydrolysis and condensation are fast, and the particles tend to rapidly compact.

Summary

In conclusion we showed in this paper how the small-angle X-ray scattering technique can be a valuable tool to provide important information about the early stage of formation and kinetic of growth of silica particles prepared by the Stöber method. Indeed, we monitored the formation of the particles and characterized the nanostructure of the particles. We found that the first particles are mass fractals and surprisingly sizable. The initial size depends on the solvent. These initial mass fractals then undergo various changes before yielding the final compact structure characteristic of these silica particles, from mass fractals to surface fractals to nonfractal particles with smooth interface. As such one can suggest that these initial mass fractals as well as the new ones can be only the primary particles. The

(30) Meakin, P. In *The Fractal Approach to Heterogeneous Chemistry: Surface, Colloids, Polymers*; Avnir, D., Ed.; John Wiley & Sons: Chichester, England, 1989.
(31) Lamer, V. K.; Dinger, R. H. *Ind. Eng. Chem.* **1950**, *72*, 4847.
(32) Lamer, V. K. *Ind. Eng. Chem.* **1952**, *44*, 1270.

models proposed so far cannot account for all these stages. In particular, one needs to pay attention to the details of what controls the initial size and the time scale of the first observable mass fractals. Here the role of the solvent is relevant.

Acknowledgment. H.B. and M.T.H. would like to acknowledge fruitful discussions with G. Beaucage. The research at the University of Maryland was supported by Start up Funds supplied to M.T.H. by the University of Maryland at College Park and the Minta Martin Aeronautical Research Fund at the University of Maryland, College Park. The research at Oak Ridge was supported by the Division of Materials Sciences, U.S. Department of Energy under Contract No. DE-AC05-96OR22464 with Lockeed Martin Energy Research Corp.

CM9702878